

# REPORT DOCUMENTATION PAGE

Form Approved  
OMB No. 0704-0188

Public reporting burden for this collection of information is estimated to average 1 hour per response, including the time for reviewing instructions, searching existing data sources, gathering and maintaining the data needed, and completing and reviewing this collection of information. Send comments regarding this burden estimate or any other aspect of this collection of information, including suggestions for reducing this burden to Department of Defense, Washington Headquarters Services, Directorate for Information Operations and Reports (0704-0188), 1215 Jefferson Davis Highway, Suite 1204, Arlington, VA 22202-4302. Respondents should be aware that notwithstanding any other provision of law, no person shall be subject to any penalty for failing to comply with a collection of information if it does not display a currently valid OMB control number. PLEASE DO NOT RETURN YOUR FORM TO THE ABOVE ADDRESS.

1. REPORT DATE (DD-MM-YYYY)		2. REPORT TYPE Technical Papers		3. DATES COVERED (From - To)	
4. TITLE AND SUBTITLE				5a. CONTRACT NUMBER	
				5b. GRANT NUMBER	
				5c. PROGRAM ELEMENT NUMBER	
6. AUTHOR(S)				5d. PROJECT NUMBER 2303	
				5e. TASK NUMBER M2C8	
				5f. WORK UNIT NUMBER	
7. PERFORMING ORGANIZATION NAME(S) AND ADDRESS(ES) Air Force Research Laboratory (AFMC) AFRL/PRS 5 Pollux Drive Edwards AFB CA 93524-7048				8. PERFORMING ORGANIZATION REPORT	
9. SPONSORING / MONITORING AGENCY NAME(S) AND ADDRESS(ES) Air Force Research Laboratory (AFMC) AFRL/PRS 5 Pollux Drive Edwards AFB CA 93524-7048				10. SPONSOR/MONITOR'S ACRONYM(S)	
				11. SPONSOR/MONITOR'S NUMBER(S)	
12. DISTRIBUTION / AVAILABILITY STATEMENT  Approved for public release; distribution unlimited.					
13. SUPPLEMENTARY NOTES					
14. ABSTRACT					
15. SUBJECT TERMS					
16. SECURITY CLASSIFICATION OF:			17. LIMITATION OF ABSTRACT  A	18. NUMBER OF PAGES	19a. NAME OF RESPONSIBLE PERSON Leilani Richardson
a. REPORT Unclassified	b. ABSTRACT Unclassified	c. THIS PAGE Unclassified			19b. TELEPHONE NUMBER (include area code) (661) 275-5015

62

separate items are enclosed

TP-FY99-0113

✓ Spreadsheet  
✓ DTS

MEMORANDUM FOR PRS

28 May 1999

FROM: PROI (TT) (STINFO)

SUBJECT: Authorization for Release of Technical Information, Control Number: AFRL-PR-ED-TP-FY99-0113  
C.W. Larson, "Kinetics of Boron Carbon HEDM"

(Statement A)

Presentation HEDM Conference

# Kinetics of Boron Carbon HEDM

C. W. Larson,  
Air Force Research Laboratory,  
Edwards AFB, CA 93524-7680

HEDM Contractors' Conference  
Cocoa Beach, FL  
7 June - 11 June 1999

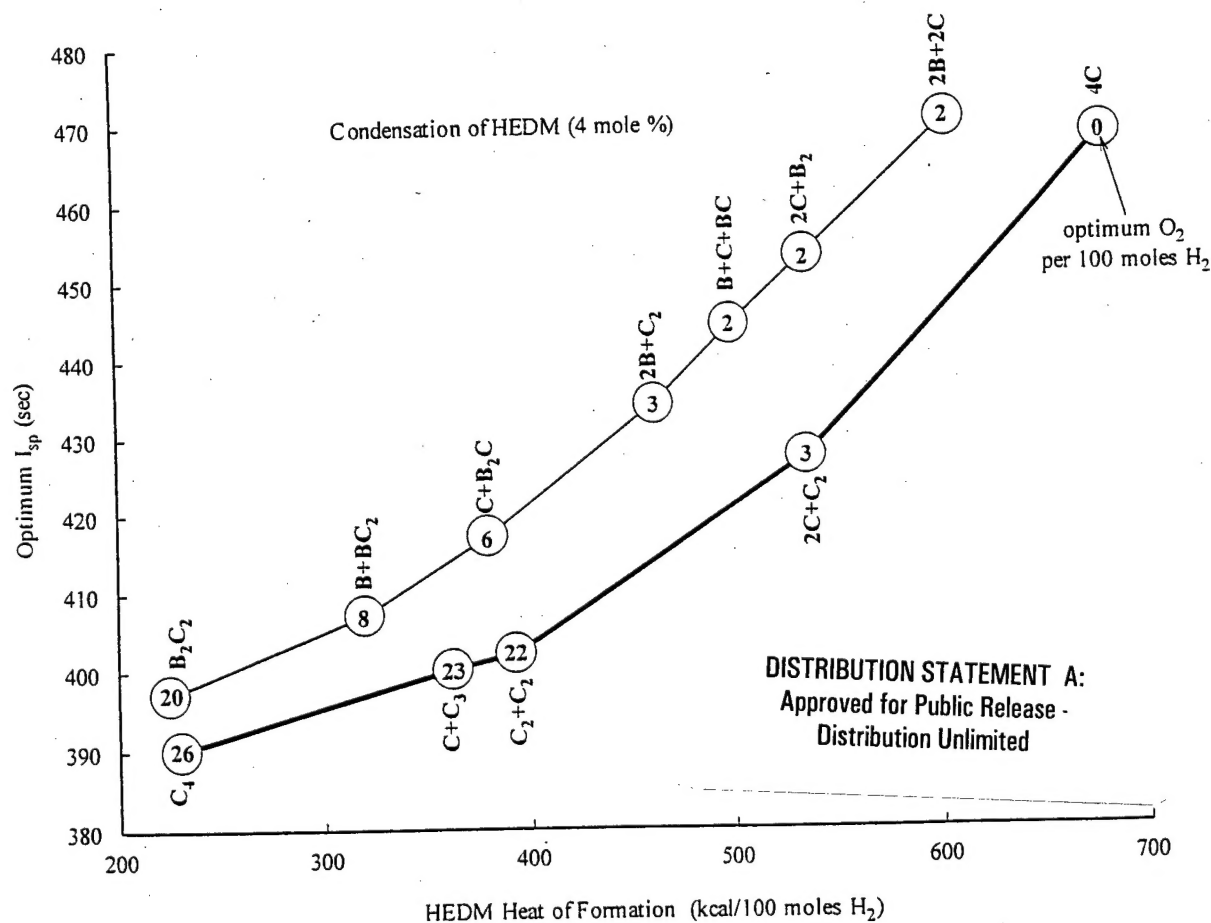


Figure 1. Specific impulse of HEDM containing 4 mole percent equivalent atom density in solid hydrogen with various stages of condensation. Numbers inside circles denote the optimum moles of O<sub>2</sub> per 100 moles of H<sub>2</sub> that produces the maximum Isp for the indicated compositions. The calculations are based on the standard rocket operating conditions, 1000 psi combustion pressure and 1 atm nozzle exit pressure, which produce 389 sec with liquid oxygen/liquid hydrogen propellant. The propellant composed of 4 mole percent C-atoms produces maximum Isp with no oxygen. If the atoms condense to 1 mole percent C<sub>4</sub>, the Isp drops to the baseline 389 sec value.

20021122 010

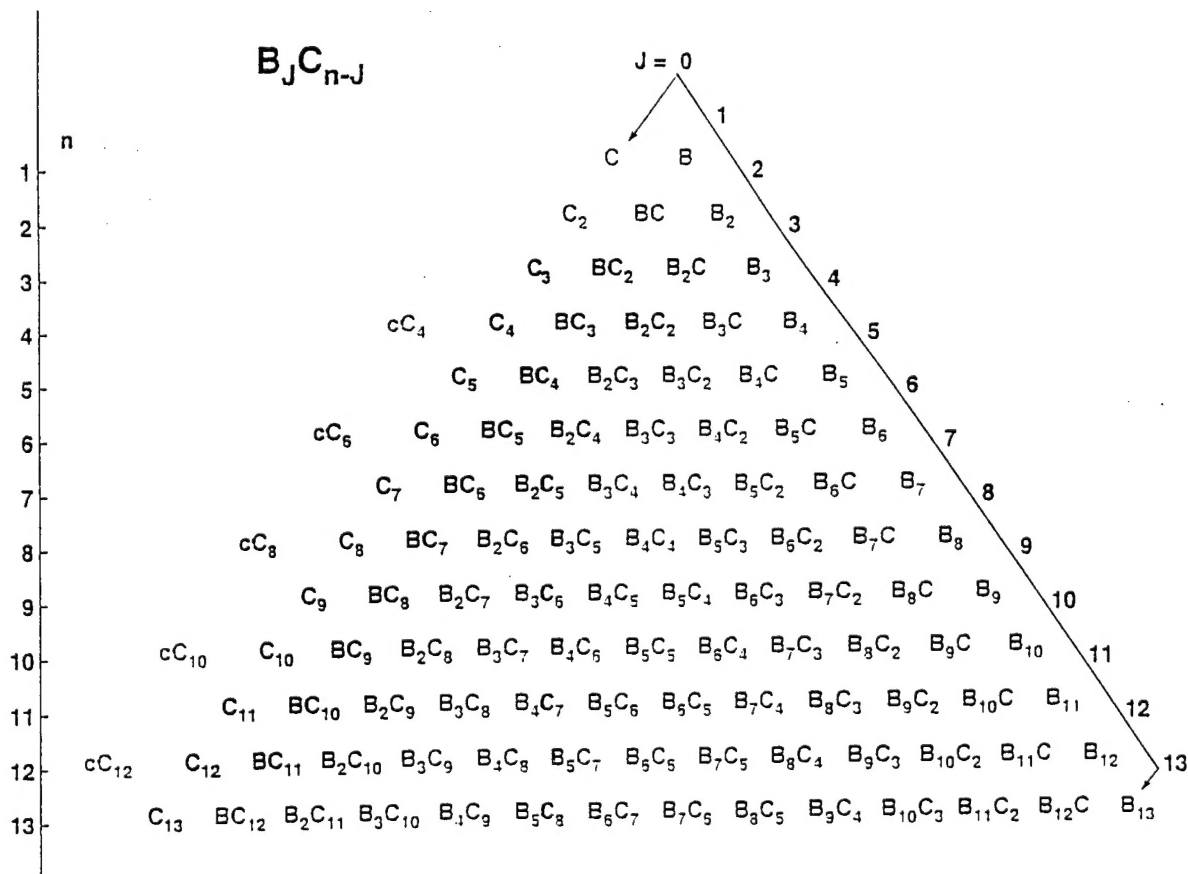
## Objective - 5% atoms in cryogenic matrix

### Approach

1. FTIR spectroscopy of  $B_J C_{n-J}$  clusters isolated in 10 K argon matrix
2. Ab-initio calculations of cluster
  - (a) normal mode frequencies and frequency shifts of their isotopomers
  - (b) infrared absorption intensities ( $\text{km mol}^{-1}$ )
3. Measurement of cluster distributions produced upon deposition and after annealing . Absolute column densities ( $\text{molecules cm}^{-2}$ ) from Beer's Law

$$\langle \rho_i I \rangle = \frac{A_{\text{exp}}}{I_{\text{theory}}} N$$

$$A_{\text{exp}} = - \int \ln \left[ \frac{E_t(\nu)}{E_0(\nu)} \right] d\nu$$



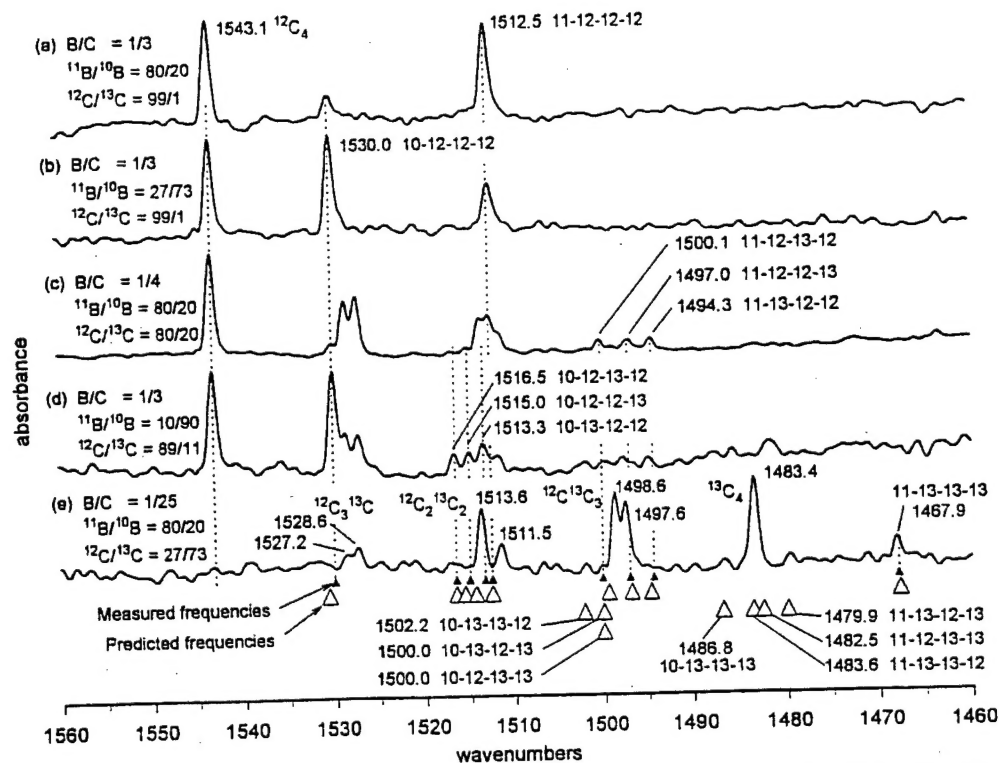


FIG. 1. FTIR spectra of the  $\nu_2(\sigma)$  mode of isotopomers of linear  $BC_4$  and the  $\nu_3(\sigma_g)$  mode of isotopomers of linear  $C_4$ . The spectra were recorded at 10 K after annealing the matrices with the indicated compositions at 27.5 K for 150 s. The large open triangles at the bottom show the predicted frequencies of linear  $BC_3$  isotopomers (as explained in the text) and small filled triangles show measured isotopomer frequencies.

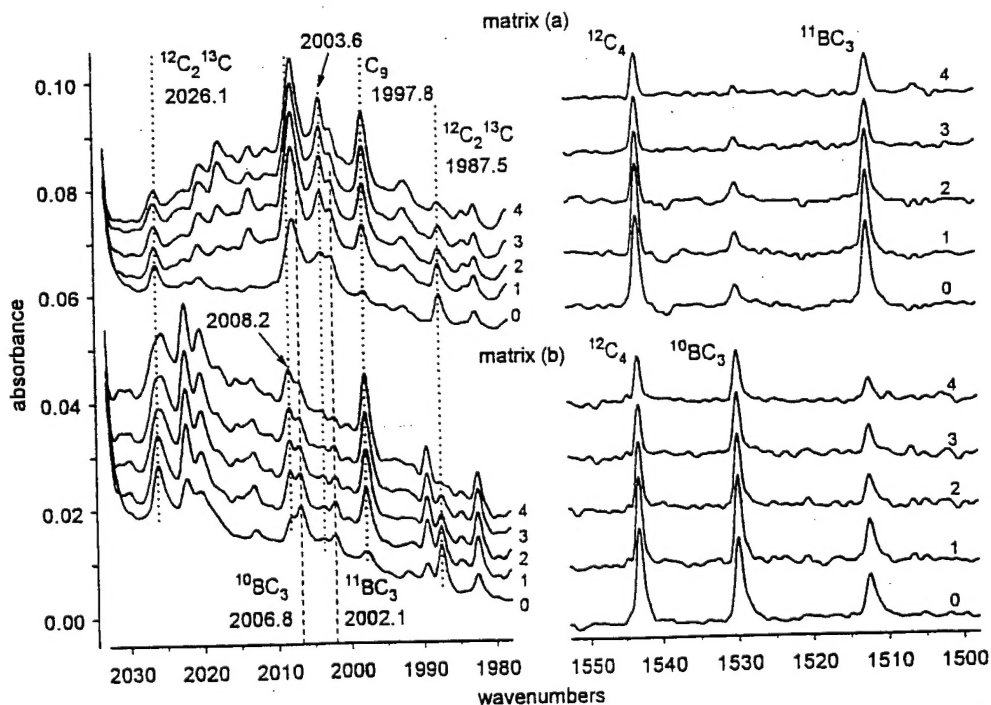


FIG. 2. Spectra obtained from matrix (a) [ $^{11}B/^{10}B = 4/1$ ] and matrix (b) [ $^{11}B/^{10}B = 1/2.7$ ] showing correlation upon annealing of the  $\nu_1(\sigma)$  bands of  $^{10}BC_3$  and  $^{11}BC_3$  at 2006.8 and 2002.1  $cm^{-1}$  with the  $\nu_2(\sigma)$  bands at 1530.0 and 1512.5  $cm^{-1}$ . The spectra labeled "0" are from the originally deposited matrix. Labels "1" to "4" indicate spectra recorded after the first through fourth annealing as follows: (1) 27.5 K for 150 s, (2) 30.0 K for 75 s, (3) 32.5 K for 45 s, (4) 35.0 K for 30 s. Frequency and absorbance scales are identical for all spectra. The plotted absorbance is  $-\log_{10}$  of the transmittance. To facilitate comparisons between matrices, the absorbance of the matrix (b) spectra are multiplied by 1.4.

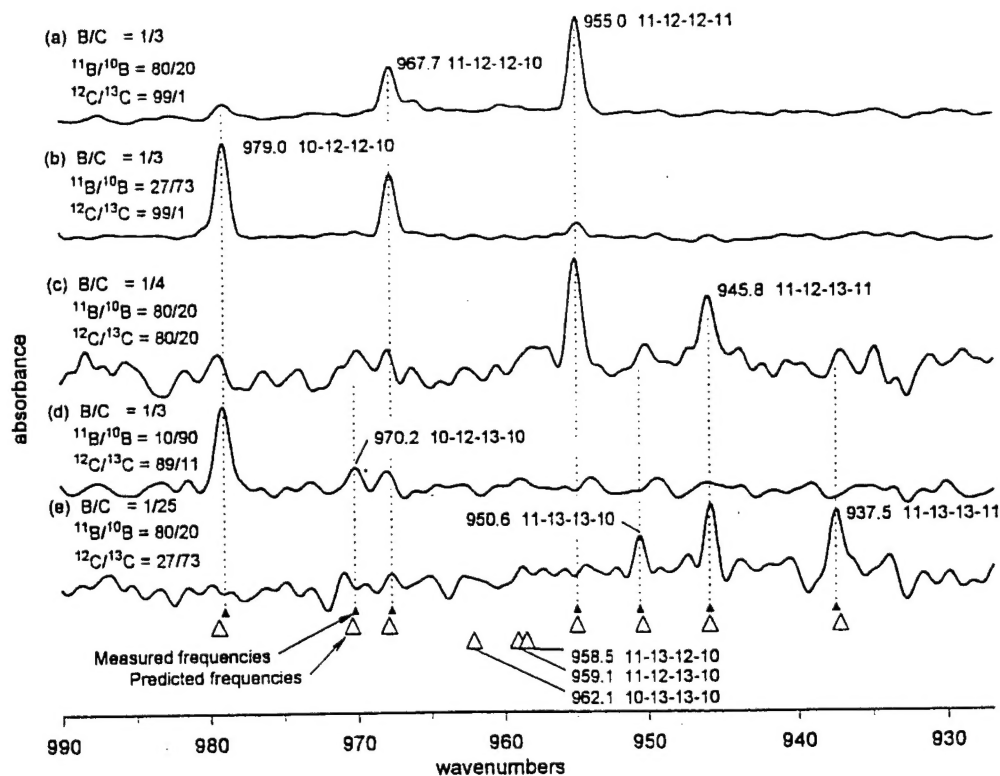


FIG. 3. FTIR spectra of the  $\nu_3(\sigma_u)$  mode of isotopomers of linear BCCB. The spectra were recorded after annealing the matrices with the indicated compositions at 27.5 K for 150 s. The large open triangles at the bottom show the predicted frequencies of linear BCCB isotopomers (as explained in the text) and small filled triangles show measured isotopomer frequencies.

TABLE IV. Experimental  $B_2C_2$  isotopomer frequency patterns. Frequencies and frequency intervals ( $\text{cm}^{-1}$ ) in triplet bands of  $B_2C_2$  isotopomers.

Boron isotope triplets				Carbon isotope triplets			
Isotopomer	Freq.	Intervals		Isotopomer	Freq.	Intervals	
		Short	Long			Short	Long
$^{10}B_2\ ^{12}C_2$	979.0			$^{10}B_2\ ^{12}C_2$	979.0	8.8	
$^{10,11}B_2\ ^{12}C_2$	967.7	11.3	24.0	$^{10}B_2\ ^{12,13}C_2$	970.2	(7.9) <sup>a</sup>	(16.7) <sup>a</sup>
$^{11}B_2\ ^{12}C_2$	955.0	12.7		$^{10}B_2\ ^{13}C_2$	(962.3) <sup>a</sup>		
$^{10}B_2\ ^{12,13}C_2$	970.2			$^{10,11}B_2\ ^{12}C_2$	967.7	(9.0) <sup>a</sup>	
$^{10,11}B_2\ ^{12,13}C_2$	(958.7) <sup>a</sup>	(11.5) <sup>a</sup>	24.4	$^{10,11}B_2\ ^{12,13}C_2$	(958.7) <sup>a</sup>	(8.1) <sup>a</sup>	17.1
$^{11}B_2\ ^{12,13}C_2$	945.8	(12.9) <sup>a</sup>		$^{10,11}B_2\ ^{13}C_2$	950.6		
$^{10}B_2\ ^{13}C_2$	(962.3) <sup>a</sup>	(11.7) <sup>a</sup>		$^{11}B_2\ ^{12}C_2$	955.0	9.2	
$^{10,11}B_2\ ^{13}C_2$	950.6	13.1	(24.8) <sup>a</sup>	$^{11}B_2\ ^{12,13}C_2$	945.8	8.3	17.5
$^{11}B_2\ ^{13}C_2$	937.5			$^{11}B_2\ ^{13}C_2$	937.5		

<sup>a</sup>Frequencies and intervals in parentheses were interpolated or extrapolated from measured quantities.

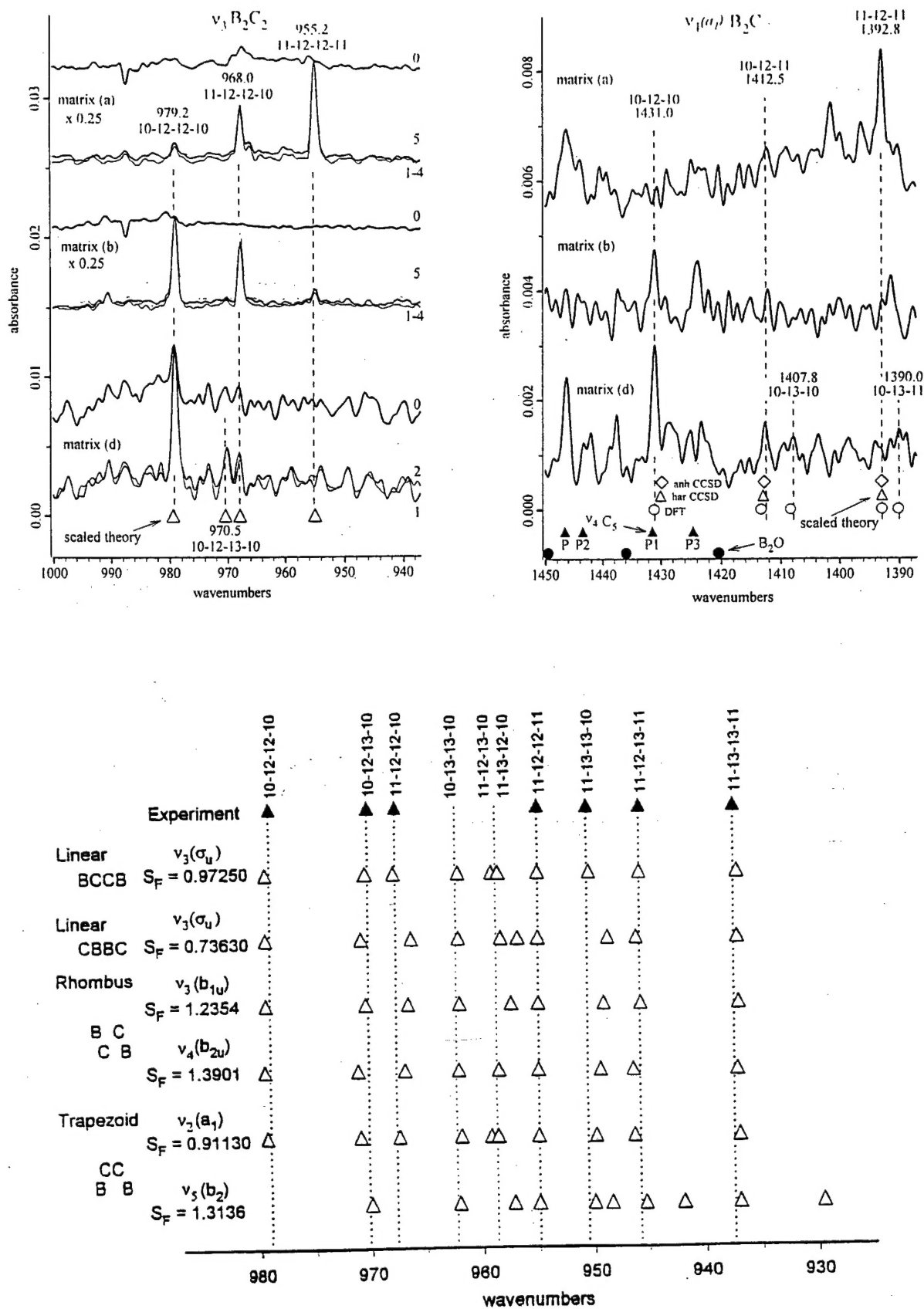


FIG. 4. Comparison of experimental isotopomer frequencies to scaled theoretical isotopomer frequencies for the most intense modes of four  $B_2C_2$  geometries as calculated by Rittby. Ref. 5.

5





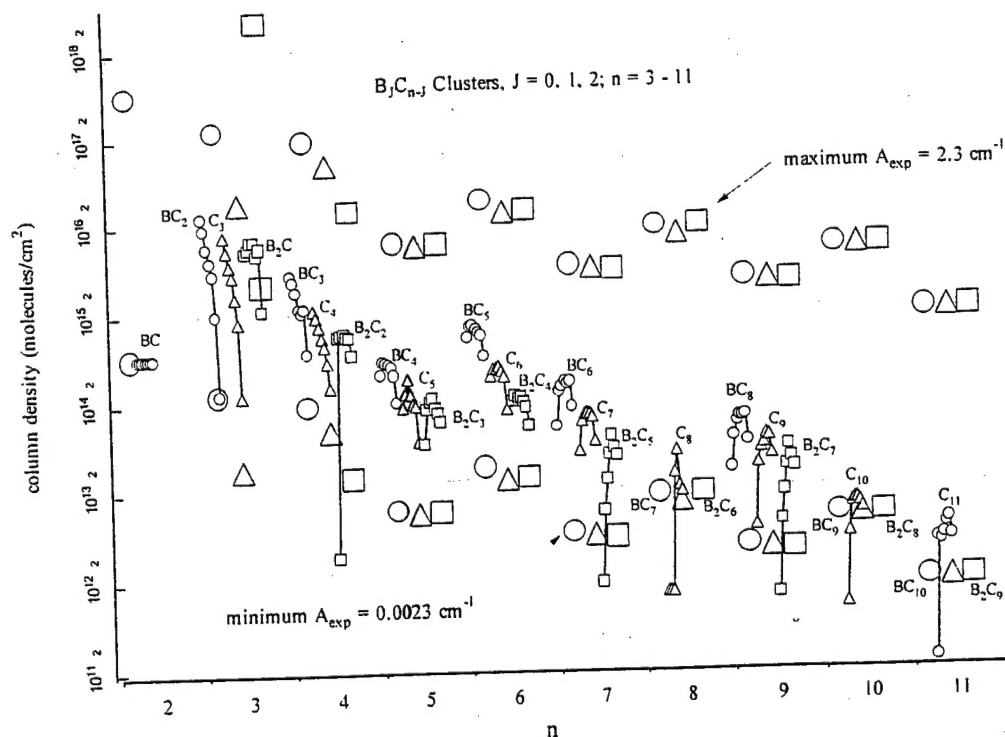
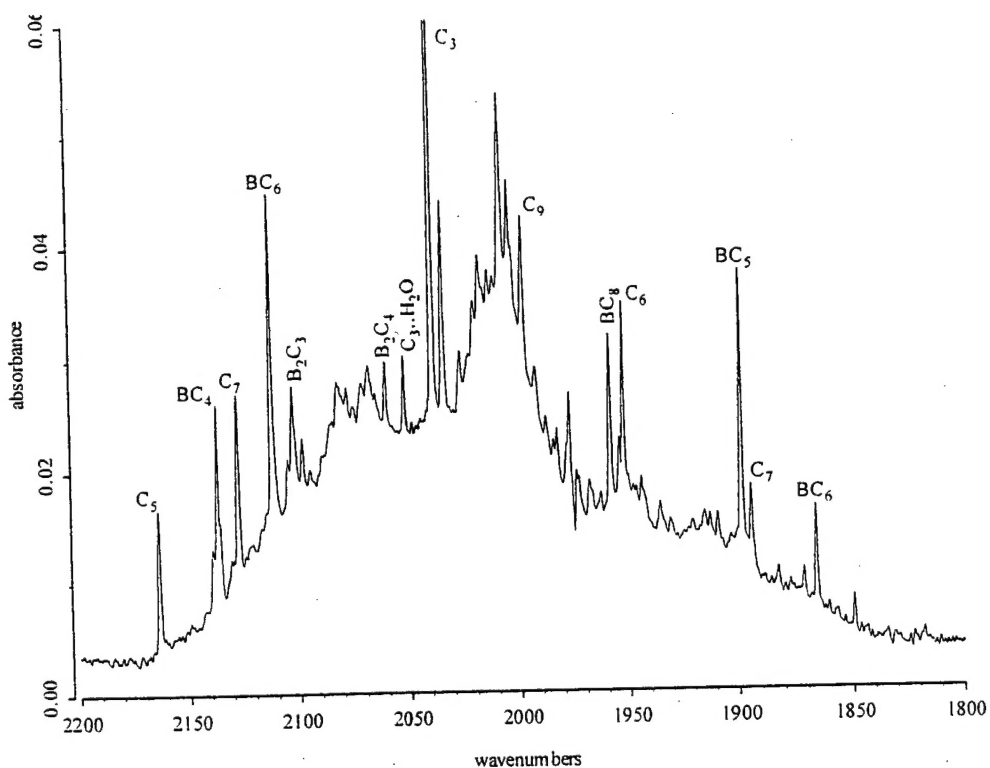
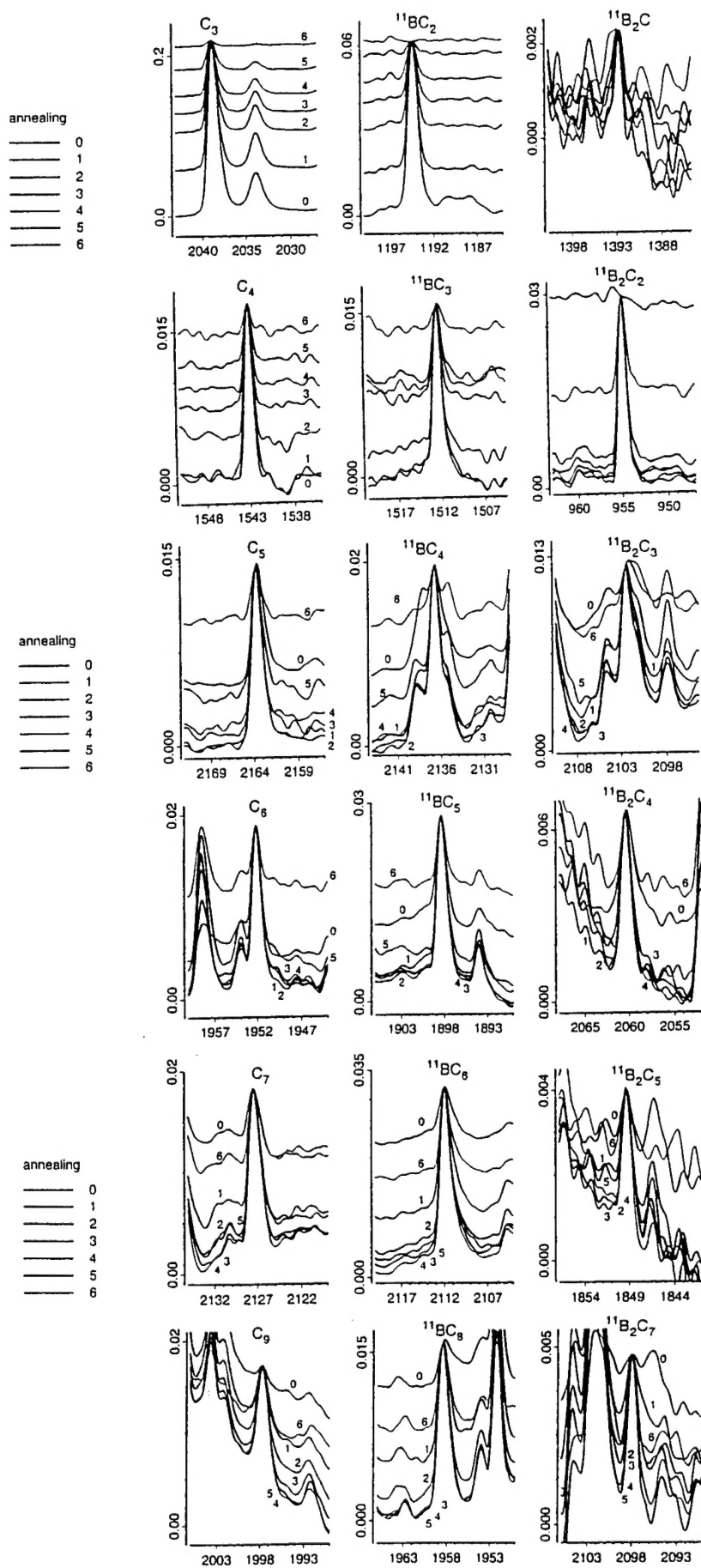
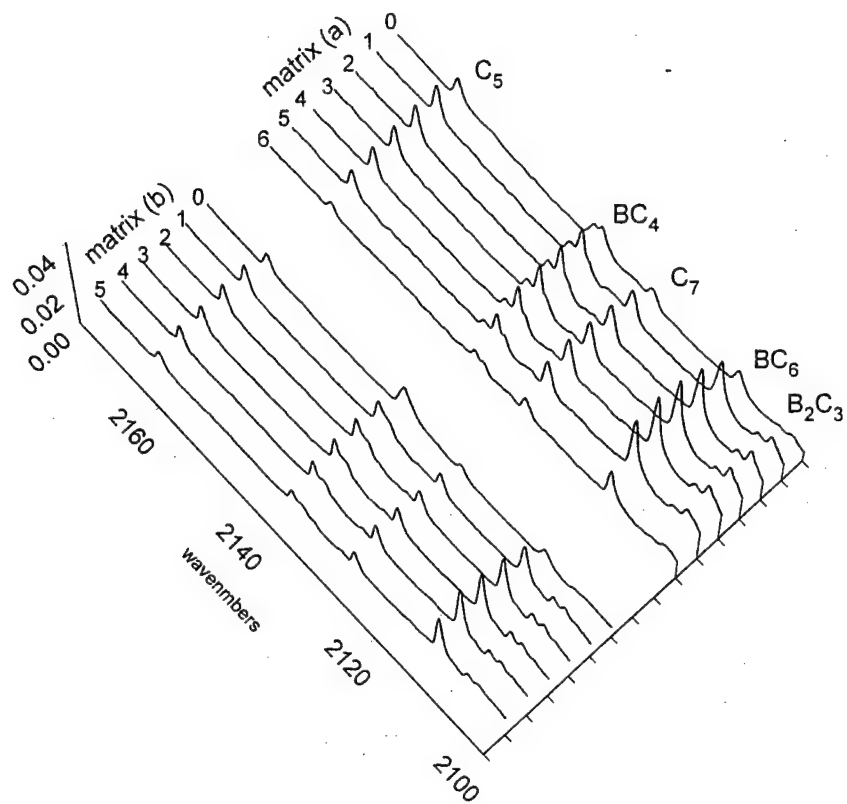


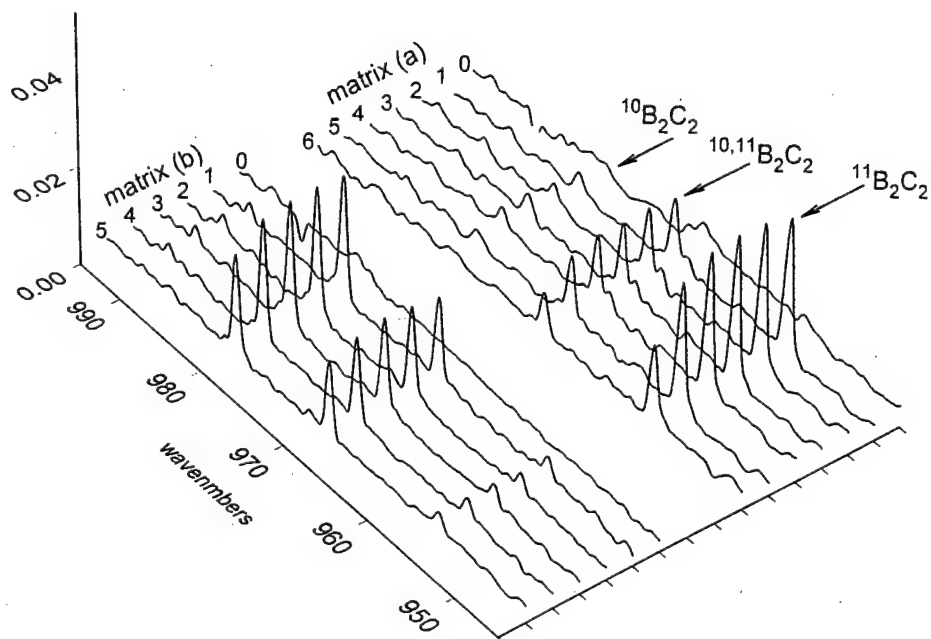
Figure 1. Distribution of  $B_nC_{n-1}$  clusters.  $J = 0, 1, 2; n = 3 - 11$ . Circles, triangles and squares represent  $BC_{n-1}$ ,  $C_n$ , and  $BC_{n-2}$  clusters, respectively. Large symbols denote upper and lower limits of measurement, based on a nominal minimum measurable absorbance of  $0.0023 \text{ cm}^{-1}$ , and a maximum absorbance for linearity of Beer's law of  $2.3 \text{ cm}^{-1}$  (1% transmittance). Small symbols denote measured quantities in the initial matrix, and in six annealed matrices. Annealing temperatures and times were (1) 27.5 K/150 s, (2) 30.0 K/75 s, (3) 32.5 K/45 s, (4) 35.0 K/30 s, (5) 37.5 K/20 s, (6) 40.0 K/20 s. The decreases in column density in the fifth and sixth annealing are due to matrix sublimation. Some of the larger clusters ( $n = 8, 10, 11$ ) have not been identified,  $BC_7$ ,  $B_2C_6$ ,  $BC_9$ ,  $B_2C_8$ ,  $BC_{10}$ ,  $B_2C_9$ .

matrix (a):  $^{11}\text{B}/^{10}\text{B} = 80/20$ ,  $^{12}\text{C}/^{13}\text{C} = 99/1$

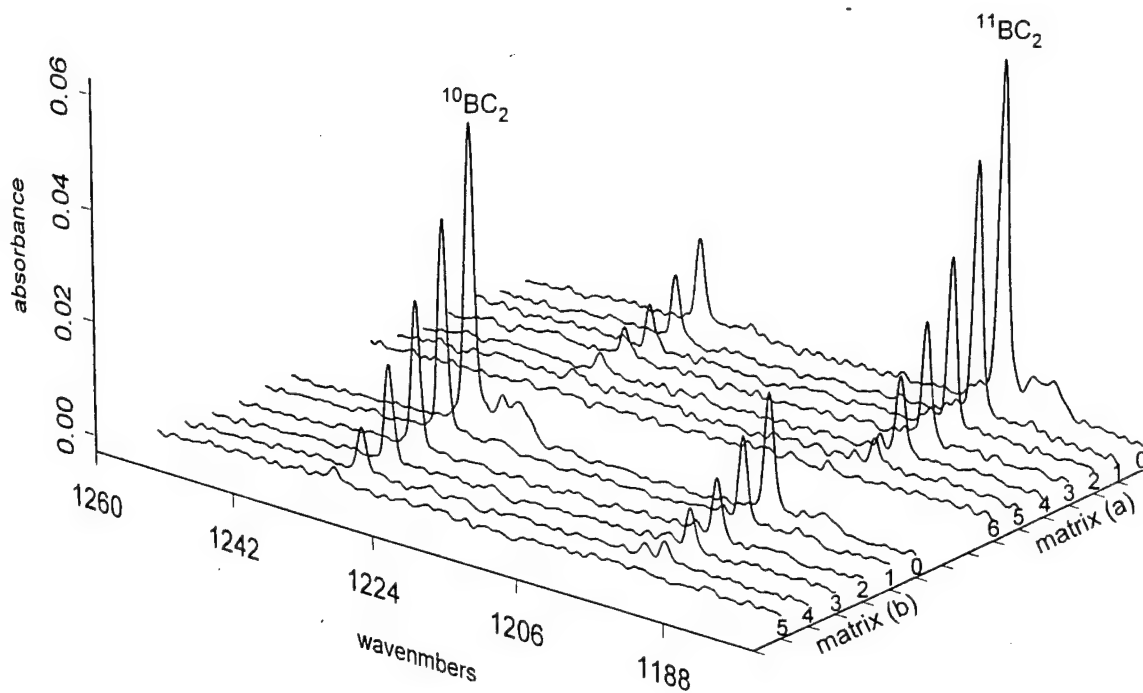




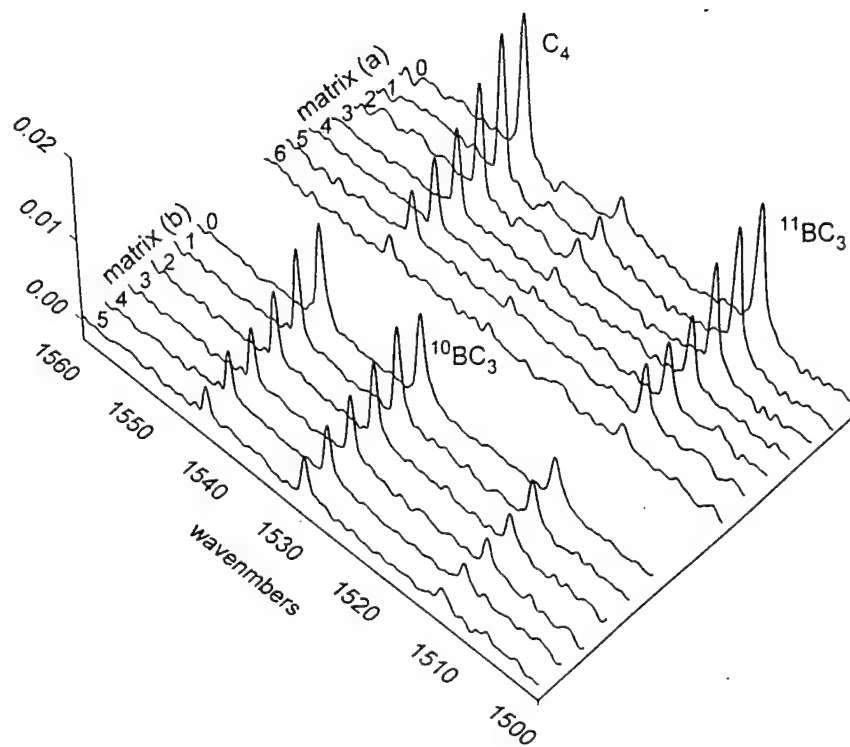
BC6rg3D May 28, 1999 8:32:14 AM



B2C2-3D May 28, 1999 8:31:14 AM



BC2rg3D May 28, 1999 8:28:17 AM



BC3rg3D May 28, 1999 8:30:29 AM

## Results and Discussion

Linear  $C_3$ , cyclic  $BC_2$ , and cyclic  $B_2C$ , constituted about 80% of the total observable boron and carbon in the initially deposited matrix, but  $B_3$  was not observed.

The measured trimer distribution in the initially formed matrices was

$$\rho(C_3) : \rho(BC_2) : \rho(B_2C) : \rho(B_3) \sim 1 : 1.5 : 0.5 : < 0.05.$$

Statistical substitution of  $J$  boron atoms into an  $n$ -atom carbon cluster produces a distribution given by  $\rho(B_J C_{n-J}) / \rho(C_n) = [\{n(n-1) \dots (n-J+1)\} / J! ] [B/C]^J$ . With the experimental  $B/C \sim 1/3$ , the statistical trimer distribution is

$$\rho(C_3) : \rho(BC_2) : \rho(B_2C) : \rho(B_3) \sim 1 : 1 : 0.33 : 0.03.$$

Agreement between distributions implies trimers form by random condensation of well-mixed atoms, uninfluenced by the relative energies of the trimers, the energies of their precursors, or preferential kinetics pathways that could otherwise distort the statistics.

Linear  $C_3$  and cyclic  $BC_2$ , disappeared entirely when the matrices were repeatedly annealed to temperatures between 25 K and 35 K, but cyclic  $B_2C$  was inert.

Linear  $C_4$  and  $BC_3$  (BCCCC) disappeared more slowly, and linear  $B_2C_2$  (BCCCB) grew to  $\sim 95\%$  of its final value during the first annealing.  $B_2C_2$  was also inert, as  $B_2C$ .

The sources of  $B_2C_2$  are from condensation of atom plus trimer ( $B + BC_2$  but not  $C + B_2C$ ) or dimer + dimer ( $BC + BC$  but not  $B_2 + C_2$ ). Although  $BC$  was not observed, the upper limit of  $\rho(BC)$  is larger than  $\rho(B_2C_2)$  so that  $BC$  cannot be ruled out as a source of  $B_2C_2$ .

The growth of  $B_2C_2$  is conclusive evidence of the presence of  $BC$  and/or  $B$  in the originally deposited matrix in an amount at least as great as the growth of  $B_2C_2$ .

Linear  $C_5$ ,  $BC_4$  ( $BCCCC$ ) and  $B_2C_3$  ( $BCCCCB$ ) and larger linear clusters ( $B_JC_{n-J}$ ,  $5 < n < 11$ ,  $J = 0, 1, 2$ ), all grew upon annealing.

The sources of  $B_2C_3$  are dimer + trimer ( $BC + BC_2$  but not  $B_2 + C_3$ ) and atom + tetramer ( $B + BC_3$  but not  $C + B_2C_2$ ).

Since  $\rho(BC_2) \sim 5\rho(BC_3)$  in the initially deposited matrix, the  $BC + BC_2$  source is dominant. Growth of  $B_2C_3$  conclusively establishes the presence of  $BC$  in the matrix in an amount at least as great as the amount by which  $B_2C_3$  grows.

Growth of  $BC_4$  occurs primarily by  $BC + C_3$  rather than  $B + C_4$  or  $C + BC_3$  because  $\rho(C_3) \sim 10\rho(C_4)$  and  $\rho(C_3) \sim 2\rho(BC_3)$ . Growth of  $C_5$  occurs by  $C + C_4$  and  $C_2 + C_3$ , which establishes the presence of  $C$  and/or  $C_2$  in the original matrix in an amount at least as great as  $C_5$  growth.

Disappearance of triangular  $BC_2$  requires breaking of one of its  $B-C$  bonds when one of its carbon atoms is attacked. The major reorganization of electronic energy involved in opening the ring appears to occur with little ( $< \sim 3$  kcal mol<sup>-1</sup>) or no energy barrier, which makes this small molecule a candidate for an interesting *ab-initio* study of unusual reactivity at low temperature.

## Goal

Production of Cryogenic HEDM with Five Mole Percent Atoms.

## Objective

Development and Characterization of Boron Atom Source.

## Approach

Production of HEDM by evaporation of boron with high-temperature graphite furnace and co-deposition of vapor with argon on a cold (10 K) surface

Identification and quantitative analysis of  $B_JC_{n-J}$  species ( $n \geq 3$ ,  $J = 0$  to  $n$ ) by FTIR spectroscopy and *ab-initio* calculations

Quantitative measurement of distributions of  $B_JC_{n-J}$  species produced upon deposition and after annealing to a constant composition.

## Summary

Identities, structures and thermodynamic properties of  $BC_2$ ,  $B_2C$ ,  $BC_3$ , and  $B_2C_2$  are conclusively established by isotope studies and matching experimental infrared spectra to predictions of theory.

Using the Standard Comparative Scheme adopted for the Isp of HEDM propellants (5 mole percent HEDM molecule in solid hydrogen) the predicted Isp of these new molecules stack up against the standards as follows:

## Summary (continued)

Isp(LOX/LH2)	389 sec
Isp(B atom)	482 sec
Isp(B <sub>2</sub> )	492 sec
Isp(BC <sub>2</sub> )	482 sec
Isp(B <sub>2</sub> C)	447 sec
Isp(BC <sub>3</sub> )	439 sec
Isp(B <sub>2</sub> C <sub>2</sub> )	439 sec

## Conclusions

Annealing kinetics of disappearance of C<sub>3</sub> and BC<sub>2</sub>, and of appearance of B<sub>2</sub>C, C<sub>4</sub>, BC<sub>3</sub> B<sub>2</sub>C<sub>2</sub>, C<sub>5</sub>, BC<sub>4</sub>, and B<sub>2</sub>C<sub>3</sub> unequivocally establishes the presence of atoms and dimers in the originally deposited matrix.

~ 80% or more of the initially deposited HEDM existed as atoms, dimers and trimers.

Molecules with two boron atoms are immune from radical attack and condensation during annealing.

## Future work

Continued development of source for production of higher flux beam of nearly pure boron atoms.

Map of "islands of stability" of pure boron HEDM; B<sub>2</sub> or B<sub>3</sub> may be the ultimate sink for atoms in the low temperature HEDM environment.

Determine reactivity of boron atoms with hydrogen during co-deposition.

Develop rapid condensation methodology to prevent reaction of B with H<sub>2</sub>.